# A DYNAMIC MODELLING OF SAFETY NETS

Yves GOURINAT
SUPAERO
10 Av E.Belin - BP54032
31055 Toulouse Cedex4, FRANCE
yves.gourinat@supaero.fr

Vincent LAPOUJADE
CRIL Technology
2, Impasse Henry Pitot
31500 Toulouse, FRANCE
vincent.lapoujade@criltechnology.com

## ABSTRACT

The nonlinear dynamic modelling of safety net systems is approached at different scales. For this purpose, the fundamental rope dynamic tests are the reference for two basic tools. One hand an anaytical bidimensional model with explicit geometrical nonlinearity and bilnear material law is proposed for preliminary design. On the other hand, a nonlinear explicit finite element is defined for numerical modelling of net systems. Semi-scale and full scale dynamic tests are performed to validate complete finite element models, suitable for global qualification of safety systems. The direct applications of these tools deal with explicit certification of safety systems for high-speed sport, such as downhill competitions.

**KEYWORDS :** Nonlinear materials - Explicit dynamics - Shock - Dynamic safety - Safety nets

## INTRODUCTION

Safety nets are at the origin of numerous structural and dynamic problematics and cover various applications, from the retention of skiers during downhill competitions to the prevention of falls in building construction. All these configurations require a high level of qualification, as human safety is involved. Therefore, robust models and in-depth comprehension of these dynamic phenomena are mandatory, in order to go on developping such systems and widen the domain of application.

The present analysis is linked to experimental processes, as each step of modelling corresponds to a specific sort of physical test. This complementarity is essential, to ensure the coherence and robustness of the structural approach, in view of certification. The fundamental analytical calculations are supported by elementary material tests, and the numerical development models are substantiated by partial scale tests. The complete model for qualification must be finally approved on the base of results obtained in full scale tests, as close as possible to real conditions of use, including environmental factors such as temperature and ageing. Fundamental modelling of the thread behavior and knot influence is mandatory, in order to ensure the reliability of the safety system design.

The models presented in this paper consider, as the reference configuration, the skier going off the piste during a competition, and retained by lateral safety nets. However, although these nets are now able to retain skiers in almost all cases, the deceleration during such impacts can cause severe harm to skiers including hyperflexion injury or vertebra compaction. Thus, for qualification requirement, it is mandatory to improve both the knowledge of dynamic rigidity of impacted fittings and the control of their intrinsic strength, in order to prevent unexpected rupture. These analyses will enable the development of diverse configurations of safety installations with the help of a computed approach, the tests being limited to the validation of algorithms and final qualification of the system. The aim of this modelling is to allow a standard dynamic qualification procedure, which has been realized and used for all new net specimens. The applications cover sport protection for competitors, but also personal safety in civil engineering, and nets for dynamic retention of freight in aircrafts, trains and trucks. For these applications, the numerical testing approach is essential, in order to minimise the costs of development and to reduce the risks. This paper presents problematics and results obtained at the laboratory of Mechanical Engineering of École Nationale Supérieure d'Ingénieurs de Constructions Aéronautiques, with the numerical assistance of Dynalis - CRIL Technology, and material cooperation of JC Dalloz Company and Centre d'Essais Aéronautiques de Toulouse, for the realization of full scale tests.

## PROBLEMATICS AND CONFIGURATION

Over the last years, the evolution of ski equipment has contributed to the increase in velocity of skiers in competitions ; security equipment should be developed consequently. It seems necessary then to analyse the quality of the safety nets that are installed along the ski slopes. When a skier loses control, he is retained by the security system. However, the strength of the impact could cause very serious damage, such as compression of vertebrae or whiplash injury.

The Figure 1 shows the complete safety system as usually found along ski slopes. The considered safety nets are made of square or diamond-shape stitches, realized with tied polyethylene cords. The net itself is surrounded by a polypropylen bolt-rope. Two taut metallic cables lock the net in translation ; the first cable is buried in the ground and linked to the net bolt-rope by static polyamid ropes, periodically disposed every 3 meters. The second rope, situated approximately 8 meters above the ground, is linked to the net by a dynamic polyamid rope, which runs in alternated pulleys. This disposition around the net absorbs a part of the impact energy. An additional polyamid tarpaulin is sometimes fixed over the net on its lower section. This avoids the cutting of the net by the sharp edges of skis at high speed. It also guides the skier towards the centre of the system, where the elasticity is higher. This is also the reason why the wall constituted by this system is not exactly vertical, but assembled with a 10 to 15 degree inclination, as shown on sketch Figure 2, in order to bring the impacting skier to the central part of the net itself, where energy absorption is more efficient.

Finally, the diverse materials used for this structure can be summarized as follows : polyethylene for the net itself, polypropylen and polyamid for surrounding attachments, and steel for external supports. The typical impact velocities vary from 10 to 30 m/s, which is comparable with a 5 to 45 m free fall.

## ELEMENTARY TESTS AND MODELLING

The basic static properties of the three types of fibers are known as follows :

| | | | Polyethylene | Polypropylen | Polyamid |
|---|---|---|---|---|---|
| Volumic Mass | $\rho$ | (kg/m3) | 408 | 620 | 1440 |
| Young's Modulus | E | (MPa) | 530 | 1740 | 5950 |
| Stress at Failure | $\sigma$ | (MPa) | 100 | 163 | 2800 |
| | | behavior | Elasto-plastic | Elastic-nonlinear | Elastic-nonlinear |

The three types of synthetic materials were tested and modelized with a special emphasis on polyethylene cords - with and without knots - which constitute the net itself. In addition, the effect of natural ageing has been taken into account by comparative tests. In these tests, new cords have been compared with identical specimens tested after 3 years' exposure to ultraviolet rays and freezing conditions on ski slopes. This study has been realized with the cooperation of F. BENYAHIA, in the frame of his specializing master in scientific computation, in order to validate dynamic data for such fibers.

***Probabilistic and Deterministic Fundamentals of Finite Element computed structural response***

Distinguishing between deterministic and random effects in Finite Element (FE) analysis structural performances is challenging. The variation of the computed structural response can be decomposed as follows :

- **Deterministic variation** : An expected, predictable, and repeatable variation in response associated with a variation in a parameter,
- **Random Variation :** Variation that cannot be associated with a change in the systems parameters. The random variation can be further decomposed as regular random variation (not known to be associated with the physics of the problem) and chaotic random variation (noise caused to grow because of bifurcation – eigenvalue – behavior in the structure).

The variation in a response due to a variation in a variable is usually known as a deterministic relationship computed using FEA. Both the variation of the structure and the variation of the environment can be described using design parameters.

Considering the sources of uncertainty in the system parameters, we can decompose the variables into two classes (using the Taguchi naming convention):

- **Control Variables :** Variables that can be controlled in the design, analysis and production, for example rope section. It can therefore be assigned a nominal value and will have a variation around this nominal value. The nominal value can adjusted in the design phase in order to have a more suitable design.
- **Noise Variables :** Variables that are difficult or impossible to control at the design and production level, but can be controlled at the analysis level; for example loads and materials variation. A noise variable will have the nominal value as specified by the distribution; that is, it will follow the distribution exactly.

The relationship between the control process variables and the response variance can be used to adjust the control variables in order to have an optimum process. The variance of the control and noise variables can be used to predict the variance of the system, which may then be used for redesign. Knowledge of the interaction between the control and noise variables can be valuable; for example, information such that the dispersion effect of the material variation (a noise variable), may be less at a high process temperature (a control variable) can be used to selected control variables for a more robust design.

With FEA, differences in modelling will give different results as well as introduce noise into the results. Amongst others, the following factors :

- Mesh density
- Choice of FE type
- Resolution of data gathered - time step and filtering selection.
- Selection of node/element to monitor,

Moreover, slightly different initial conditions, especially when driven by eigenvalues, can lead to noticeable differences in responses.

- **Mechanical behaviour :**
  - o Bifurcation events can be sensitive to initial values; for example, buckling initiation.
  - o Changes in the design variables may cause different components to come into contact, or change the order of impact.
- **Algorithmics :**
  - o Contact algorithms. The discretization of a smooth structure into piecewise linear finite elements may lead to different orders of events; for example, a node impacting the edge of a given element may impact the edge of its neighboring element in a similar simulation.

At each step of the model building, the problem is ivestigated using a parametric study in which we vary one of the variables at a time. Considering the analysis of the results, it is clear that this impact problem, involving both material and geometrical non linearities, leads to a limited number of bifurcation points, and small noise.

### *Static longitudinal behavior of cords*

The static characteristics of the cords are obtained using a comparison-correction method between experimental data and simulation, in which stress-strain profiles are compared. A specific facility has been developped, which avoids stress concentration at attachement points. The tensile test machine pulls two thick cylinders, around which the tested cord is wound. Figure 3 shows the corresponding model on explicit Finite Element, modelizing the cord by elasto-plastic approximation, and the rest of the fixture by rigid elements. In accordance with the material configuration, the explicit model considers one fixed cylinder, and one mobile cylinder.

The tensile test leads to a parametric study in which each parameter is fixed separately. Among the large number of parameters taken into consideration, the following were specifically investigated : beam formulation, number of beam elements for the cord, contact algorithm type, relative mesh density of cylinder and cords, tensile test speed, material law for the cord. Using a simple comparison-correction method in concordance with parametric study to evaluated noise variables effects, we finally converged to a material law, mesh density, element type, contact type and relative mesh density for the FE model.

The model calculates directly the nodal displacements, the stresses in elements, and integrates the total strain energy. The elasto-plastic parameters of the ropes in numerical model have been adjusted to represent the absorbed energy. This energy, integrated in tests from tensile force with displacement, is shown in Figure 4 for polyethylene cord. The modelized absorbed energy in the cord fits with the experimental curve. It is also necessary to mention that the presence of knots on the cord (Figure 5), and its ageing, have been taken into account, as the tests dealt with real knotted and aged specimens. These perturbations modify the parameters in a range of 15%, which does not change the nature of phenomena but causes the simulation to stop earlier by rupture, the failure threshold being significantly lower.

### *Dynamic behavior of cords*

The next step consisted in modelling with good accuracy and robustness the dynamic absorption of energy in net cords. For this purpose, lateral impact tests were performed on a cord at various speeds from 2.5 to 6.4 m/s, with a 5kg and 14mm diameter impactor. The Figure 6 shows the impact device used for test and the Figure 7 shows the associated numerical model. This explicit finite element model implies 1153 elements, including 234 beam elements for the cord itself. The lateral 95mm diameter aluminium cylinders, and the impactor itself are represented by tridimensional rigid elements, with 0.3 sliding ratio.

During the tests, displacement and acceleration of the impactor were recorded. The same kind of parametric study was conducted for the dynamic tests modeling. The conclusions from the first model were investigated more precisely to detect any behavior modification due to dynamic aspect of the response. A short analysis of experimental data leads to modify the material law using a non linear approach. Different models were tested (non linear elastic, elastic plastic,…). The elastic perfectly plastic approach leads to a good compromise in terms of precision with a simple model for the expected impact velocity range.

The Figure 8 shows the results in terms of impactor acceleration. The material parameters obtained here lead to a correct estimation of the polyethylene cord performance. After the static adjustement, based on the tensile test, the present modelling proves its capability to represent the dynamic effects of impact on actual transverse computation. The material behavior of polyethylene cord is adjusted in accordance with a bilinear law, considering kinematic strain-hardening with the following values :

| | | | |
|---|---|---|---|
| Young's modulus : | $E$ | 387 | MPa |
| Elastic limit : | $\sigma_y$ | 124 | MPa |
| Tangent Module : | $E_t$ | 0 | MPa |
| Poisson's ratio : | $\nu$ | 0.4 | |

More precisely, the results obtained with these values provide the following precision, in relation with the dynamic lateral test :

| | Impact velocity | 2.5 m/s | 4.43 m/s | 5.56 m/s | 6.41 m/s |
|---|---|---|---|---|---|
| Computation result | Acceleration | -1% | -0,02% | -0,06% | -7% |
| compared with measures | Deflection | 5% | 4% | 5% | 3% |

***Preliminary semi-scale net test***

Thanks to this lateral dynamic test and computation, the elementary mechanism for net energy absorption has been modelled, which provided a global modelling of the fixture. It was then necessary to define a configuration for qualification. This has been made in the frame of S. ERIKSSON's internship at ENSICA, under the auspice of the Erasmus European Student Exchange. A preliminary square 1.5mx1.5m net, directly and simply supported on a horizontal square metallic frame, has been tested in ENSICA's facilities, with a 27 kg aluminium spherical mass dropped from 3.30m above the net (impacting speed : 8m/s). This semi-scale test helped to define the final full-scale configuration, which is now presented.

Due to simple boundary conditions and the relative small size of the model, a large number of simulations were done still using a parametric study in which we vary one of the variables at a time. All the conclusions from the two previous models were reinvestigated to capture any new unexpected behavior due to the more complex configuration.

## QUALIFICATION STRUCTURAL TESTS AND MODEL

In order to validate the whole safety system model, impact tests were performed on complete net sections. Both square and rhombus nets were used, constituting a 3m x 3m square surface, supported on an external metallic frame (5m x 5m) with bolt-ropes. It was impacted by a 100 kg (400 mm diameter) hollowed aluminium sphere at different vertical velocities between 4.4 and 10 m/s (dropping heights from 1 to 5.1 m). Figure 9 shows the experimental facility and Figure 10 shows the corresponding model. During this campaign, 12 drop tests were performed on this facility, allowing a reliable modelisation of the net itself with its surrounding bolt-rope. Only 8 specimens were tested, as one was impacted two times at the same speed, and another one 4 times at increasing speeds.

The validation of numerical modelling of the net element is founded on the comparison between computed and measured values in fundamental initial impact comfiguration, dealing with the 100 kg spherical mass vertically impacted on the net. The four referenced configurations can be summarized as described in the following table :

| Impacts on 3x3m polyethylene net Referenced cases definition | | | | | |
|---|---|---|---|---|---|
| Referenced case | Impact | | | Net | |
| | Weight (kg) | Direction | Speed (m/s) | Configuration | Stitch |
| #1R | 100 | Vertical Down | 4,43 | Frame 3x3m | Rhombus |
| #1S | 100 | Vertical Down | 4,43 | Frame 3x3m | Square |
| #2R | 100 | Vertical Down | 9,51 | Frame 3x3m | Rhombus |
| #2S | 100 | Vertical Down | 9,90 | Frame 3x3m | Square |

The full simulation frame (element type, number of element per cord between to knots, material laws, contact type, …) developed for the semi-scale net were used for full scale modeling. Based on previous material laws, the numerical computations are compared with experimental results as follows :

Impacts on 3x3m polyethylene net : Computed values and test data

| Case | *Results* | **Maximal deflection at impact point** | | **Maximal acceleration at impact point** | |
|---|---|---|---|---|---|
| | | Value (mm) | Time (ms) | Value (G) | Time (ms) |
| #1R | *C : Computed* | 870 | 220 | 7 | 220 |
| | *M : Measured* | 813 | 210 | 6,6 | 200 |
| | ***(C-M)/M*** | **7%** | 5% | **6%** | 10% |
| #1S | *C* | 836 | 215 | 6,9 | 205 |
| | *M* | 813 | 210 | 6,7 | 190 |
| | ***(C-M)/M*** | **3%** | 2% | **3%** | 8% |
| #2R | *C* | 1195 | 168 | 16 | 165 |
| | *M* | 1296 | 160 | 14,9 | 160 |
| | ***(C-M)/M*** | **-8%** | 5% | **7%** | 3% |
| #2S | *C* | 1183 | 156 | 16,3 | 155 |
| | *M* | 1181 | 160 | 16,6 | 150 |
| | ***(C-M)/M*** | **0,2%** | -2% | **-2%** | 3% |

The #2R was performed near the limit of failure : the rhombus stitch leads to failure at 9.90 m/s speed, in 3x3m frame configuration. The failure at 9.90 m/s has been obtained in test and computing, as shown on Figure 11 (model) and 12 (computed accelerations). Thus, the more critical case for which the model has been actually validated is therefore #2S. For this case, Figure 13 presents the evolution of the energies in the model. The following points may be observed on this figure :

- the sum of Kinetic and Strain energies increases up to the weight potential due to gravity at maximal deflection ; should the test be performed in a horizontal direction, this total energy would be constant, the kinetik energy being converted in strain ;
- the sliding energy is maximal when the elongation is maximal, but remains very small (less than 1/1000th of the total energy) ;
- the hourglass energy, generated by unconventional deformation of elements, is totally negligible.

This energetical approach and criterion constitutes a classical way to validate from a pure numerical point of view an explicit simulation result keeping in mind our engineering judgment. The precision of the FE model was considered as sufficient for further predictive analyses.

## ADDITIONAL RESULTS OF COMPUTATIONS

The numerical model is used to compute different configurations. The first computation considers variable speeds with constant kinetik energies. For this purpose, case #1S with 3x3m frame has been recomputed with horizontal motion, more closely representing the skier stopped by a net. The considered cases are summarized hereunder :

| 3x3m polyethylene net speed test | | | | | |
|---|---|---|---|---|---|
| Case | Impact | | | Net | |
| | Weight (kg) | Direction | Speed (m/s) | Configuration | Stitch |
| #3L | 100 | Horizontal | 4,43 | Frame 3x3m | Rhombus |
| #3H | 20 | Horizontal | 9,90 | Frame 3x3m | Rhombus |

Figure 14 shows the computed deflections for these two cases, and Figure 15 shows the accelerations. These figures show clearly that the maximal elongation is practically constant, corresponding to the absoption of the same kinetic energy by the net. The difference consists in the time of deceleration, which is significantly shorter for the small mass, inducing higher levels of acceleration.

### *Complete net-system computation and test*

The net itself being modelized with the adequate precision, the complete model is then performed with surrounding structures, representing a real section of operational nets. Thus, a second series of tests is performed, with surrounding ropes and cable-pulleys, with following significant cases :

| Impacts on 3x1.5m polyethylene net with complete surrounding facility | | | | | |
|---|---|---|---|---|---|
| Case | Impact | | | Net | |
| | Weight (kg) | Direction | Speed (m/s) | Configuration | Stitch |
| #4R | 100 | Vertical Down | 9,47 | Frame+pulleys | Rhombus |
| #4S | 100 | Vertical Down | 9,44 | Frame+pulleys | Square |

The frame fixture being unchanged, the size of the net itself is then reduced to a 3mx1.5m rectangle. The same kind of parametric study was conducted both for surrounding rope and the cable–pulleys modeling. Figure 16 shows the numerical model, corresponding to test configuration represented on Figure 17. In addition, Figure 18 shows the detailed representation of a pulley and net edging, with two elements for each stitch-side.

The computation is compared with experimental results in the table herunder :

| Complete net facility : Computed & test values at impact point | | | | |
|---|---|---|---|---|
| Case | *Results* | Maximal deflection (mm) | Maximal speed (m/s) | Maximal acceleration (m/s2) |
| #4R | *C : Computed* | 1361 | 9,78 | 20 |
| | *M : Measured* | 1374 | 9,83 | 14,2 |
| | ***(C-M)/M*** | **-1%** | **-1%** | ***41%*** |
| #4S | *C* | 1246 | 9,69 | 17,2 |
| | *M* | 1243 | 9,87 | 17,3 |
| | ***(C-M)/M*** | **0,2%** | **-2%** | **-1%** |

The precision of the global numerical explicit modelling is acceptable, except for the computation of the maximal acceleration in the case of rhombus stitching. This is due to local failures in various places, this test being at the limit of global failure. These local failures are observed on the acceleration curve presented in Figure 19, with local picks and irregularities. In addition, the analysis of the evolution of energies shows clearly that the sliding energy is no longer negligible, but represents 3% of the total energy at the end of the simulation (see Figure 20).

## ANALYTICAL APPROACH

In this paragraph, an analytical approach of the elementary mechanism of geometrical nonlinearity of the net is proposed, allowing a restitution of the first phase of deceleration. The basic configuration is described as follows :

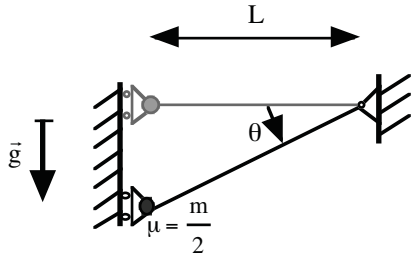


The mass of the net itself is supposed to be much smaller than the impacting mass m. In the real facilities, the net moving section represents approximately 2% of the skier mass. The considered reference cases are #2S and #4S, with symmetrical square stitching. The first one deals with the net itself, and the second one tests the equivalence with the global system including net and supports.

The mechanical conservative energy, including the weight potential and the kinetic energy, is given by :

$$2\left(\mathcal{E}_{mg}+\mathcal{E}_{kin}\right)=\mu\left[-2gL\tan\theta+\left(L\frac{d}{dt}\tan\theta\right)^2\right]$$

Then, to compute the strain energy, it is necessary to consider an assumption on the relation between the bar elongation and its load. If this relation is considered as linear, with k ratio constant (linear bar), and if the bar is constituted of a linear material whose equivalent module is E, with constant S cross section, the strain energy is given by :

$$2\,\mathcal{E}_{\text{lin bar}}=kL^2\left[\frac{1}{\cos\theta}-1\right]^2=ESL\left[\frac{1}{\cos\theta}-1\right]^2$$

This model is nonlinear only in terms of geometry, but allows a simple expression of the energy. The total energy is conserved during the motion, and remains equal to its initial value, defined as follows :

$$\text{at } t_0 = 0,\ \theta = 0,\ E_{\text{total }0} = E_{\text{kin }0} = \frac{m}{4} V_{\text{impact}}^2$$

Thus, the conservation of energy is expressed as follows :

$$\frac{mL^2}{4}\frac{\dot{\theta}^2}{\cos^4\theta} - \frac{m}{2} gL\tan\theta + \frac{ESL}{2}\left[\frac{1}{\cos\theta} - 1\right]^2 = \frac{m}{4} V_{\text{impact}}^2$$

This equation explicitely expresses the angular speed $\dot{\theta}(t)$ in function of $\theta(t)$.

In order to compare with Finite Element computation, based on reference case #2S, the maximal elongation point is considered. This value $\theta_{max}$ of $\theta$, considered as the adjustment point, is defined for case #2S by :

$$\tan(\theta_{max}) = \frac{L_{max}}{L} = \frac{1183\ \text{mm}}{1500\ \text{mm}} \cong 0.789$$

This value is used to define the equivalent fiber cross section which will be considered for the computation. This section is such as the speed is zero when $\theta$ reaches its maximal value, as follows :

$$S_{lin} = \frac{\left[\frac{mV_{\text{impact}}^2}{2L} + mg\tan\theta_{max}\right]}{EL\left[\frac{1}{\cos\theta_{max}} - 1\right]^2}$$

Consequently, considering the dimension ot the net, the numerical values to be consdered in this analytical approach are : L=1.5m, m=100kg, g=9.81ms$^{-2}$, E=387MPa, $V_{impact}$=9.9ms$^{-1}$. With these values, the equivalent cross section is :

$$S = 93.0\ \text{mm}^2$$

Then, the maximal impactor acceleration is calculated by vertical projection at maximal elongation :

$$\Gamma_{max} = \frac{\left[ES\left(\frac{1}{\cos\theta_{max}} - 1\right)\sin\theta_{max} - \frac{mg}{2}\right]}{\frac{m}{2}} = 2ESL\left[\tan\theta_{max} - \sin\theta_{max}\right] - g$$

With the simplified linear material, the value found for this maximal acceleration is 11.43G, which is 30% lower than the 16.30G reference value. Thus, the geometrical nonlinearity has to be combined with material nonlinearity.

The material nonlinearity is represented in the analytical model as stress truncature, as follows :

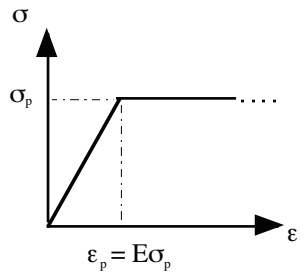


This simple model allows a first step approach of initial impact dynamics ; the material non-linearity has been modelled by its stress-truncating effect, corresponding to plastic threshold. This model is obviously limitated to primary dynamic strain ; it cannot simulate the spring-back effect after maximal extension. In fact, it is adapted to initial design for maximal load and extension in nets.

Therefore, in this model, the material remains linear for $\theta \le \theta_p$ defined as follows :

$$\delta L_p = L\left(\frac{1}{\cos\theta_p} - 1\right) \Rightarrow \frac{\delta L_p}{L} = \varepsilon_p = \left(\frac{1}{\cos\theta_p} - 1\right) \Rightarrow \cos\theta_p = \frac{1}{1+\varepsilon_p} = \frac{E}{E+\sigma_p}$$

Consequently, for $\theta \le \theta_p$, when the material is plastified, the expression of the conservation of energy becomes :

$$\frac{mL^2}{4}\frac{\dot{\theta}^2}{\cos^4\theta} - \frac{m}{2}gL\tan\theta + \frac{ESL}{2}\left[\frac{1}{\cos\theta_p} - 1\right]^2 + ESL\left[\frac{1}{\cos\theta_p} - 1\right]\left[\frac{1}{\cos\theta} - \frac{1}{\cos\theta_p}\right] = \frac{m}{4}V_{impact}^2$$

It is then possible to recalculate the equivalence cross section which allows, with bilinear assumption, to stop the mass at $\theta = \theta_{max}$ :

$$S_{bilin} = \frac{\left[\frac{mV_{impact}^2}{2L} + mg\tan\theta_{max}\right]}{EL\left(\frac{1}{\cos\theta_p} - 1\right)\left[\left(\frac{1}{\cos\theta_p} - 1\right) + 2\left(\frac{1}{\cos\theta_{max}} - \frac{1}{\cos\theta_p}\right)\right]}$$

Finally, after this preliminary calculation, it is possible to integrate the motion, thanks to the explicite expressions : $\theta = \theta_{max}$ :

$$\begin{cases} \text{For } 0 \le \theta \le \theta_p : \dot{\theta}_I^{\,2} = \dfrac{2\cos^4\theta}{L^2}\left[\dfrac{V_{impact}^2}{2} + gL\tan\theta - \dfrac{ESL}{m}\left[\dfrac{1}{\cos\theta} - 1\right]^2\right] \\ \text{For } \theta_p \le \theta : \dot{\theta}_{II}^{\,2} = \dfrac{2\cos^4\theta}{L^2}\left[\dfrac{V_{impact}^2}{2} + gL\tan\theta - \dfrac{ESL}{m}\left(\dfrac{1}{\cos\theta_p} - 1\right)\left[\left(\dfrac{1}{\cos\theta_p} - 1\right) + 2\left(\dfrac{1}{\cos\theta} - \dfrac{1}{\cos\theta_p}\right)\right]\right] \end{cases}$$

In particular, this step by step procedure allows the explicit computation of the deflection and velocity according to the time.

These analytical results are summarized in the following table, and compared with Explicit Finite Element reference computation :

| Explicit analytical approach with linear and bilinear bar (case #2S) | | | | |
|---|---|---|---|---|
| | Maximal deflection (mm) | Maximal acceleration (G) | Time at Maxi.deflection (ms) | Observation |
| Analytical Linear Bar | 1183 | 11,43 | 174 | E=387MPa |
| Explicit Finite Element | 1183 | 16,30 | 156 | S=87.6 mm2 |
| Relative Difference | (reference) | ***-30%*** | ***12%*** | |
| Analytical Bilinear Bar | 1183 | 16,30 | 150 | E=387MPa |
| Explicit Finite Element | 1183 | 16,30 | 156 | S=140,4 mm2 |
| Relative Difference | (reference) | ***0%*** | ***-4%*** | Plast.stress : 97.6 MPa |

The precision is acceptable in terms of deflection and acceleration levels, but the shape of velocity curves shows clearly a 30% difference (see figure 21), which confirms that the analytical approach is suitable only for preliminary sizing.

## CONCLUSION

The contribution presented in this paper provides two complementary approaches of net dynamic modelling, both of them being based on bilinear material law. The first approach consists in an analytical two dimensional methodology for preliminary design and computation, with explicit energy equations. The second one is an explicit numerical modelling which has been validated for the qualification of nets, on the basis of normalized tests at various scales. The stake of this qualification is obviously significant for the dynamic safety of nets in these diverse applications in sport competitions. The assumptions and numerous tests and numerical runs allow a good robustness of the approach, which make possible the qualification of these dynamical systems by computation.

**ACKNOWLEDGEMENTS :**

M. J-C DALLOZ for net specification and Mrs. Isabelle BANEL for full-scale test specification
MM. M LABARRERE and F BEN YAHIA, ENSICA, for laboratory material tests
CRIL Technology for numerical model support
CEAT for full scale test realisation

**REFERENCES :**


[1] Z. Ren and M. Vesenjak, *Computational and experimental crash analysis of the road safety barrier* - Engineering Failure Analysis 12 (2005) (6), pp. 963–973, 2005.

[2] M. Borovinsek, M. Vesenjak, M. Ulbin and Z. Ren, *Simulation of crash tests for high containment levels of road safety barriers* - Engineering Failure Analysis, In Press, Corrected Proof, Available online 30 January 2007.

[3] Benson, D.J. and Hallquist, J.O, *A Single Surface Contact Algorithm for the Post-Buckling Analysis of Structures* - Computer Methods in Applied Mechanics and Engineering, Vol. 78, pp. 141-163, 1990.

[4] Hallquist, J.O., Goudreau, G.L. and Benson, D.J., *Sliding Interfaces with Contact-Impact in Large-Scale Lagrangian Computations* - Computer Methods in Applied Mechanics and Engineering, Vol. 51, 107-137, 1985.

[5] Sims, G.L.A. and Pentrakoon D., *Initial impact studies on open and closed cell foam foams* - Cellular Polymers, 16, 431-443, 1997.

[6] P. du Bois, T. Frank, *Crash Simulations of Hat Sections – Reliability of the Numerical Model* – 3rd European LSDYNA Users Conference, Paris 2001.

[7] W. Roux, N. Stander, *Analysing "Noisy Structural" Problems with LS-OPT: Probabilistic and Deterministic Fundamentals* – 4th European LSDYNA Users Conference, Ulm 2003.

[8] G. Blankenhorn, K. Schweizerhof, H. Finckh, *Improved Numerical Investigations of a Projectile Impact on a Textile Structure* – 4th European LSDYNA Users Conference, Ulm 2003.

[9] A.I. Borovkov, I.B. Voinov, *FE Analysis of Contact Interaction Between and Woven Structure in Impact Process Rigid Ball* – 8th International LSDYNA Users Conference, Detroit 2004.

[10] G. Lyn, N. J. Mills, *Design of foam crash mats for head impact protection.* - Sports Engineering - Volume 4 Page 153-163 - August 2001 -Issue 3.

[11] European Standard French Version – Association Française de Normalisation (AFNOR).
- [11.1] DIN EN 564 – *Mountaineering equipment - Accessory cord - Safety requirements and test methods* (NF EN 564, June 2005).
- [11.2] NF EN 892- *Equipement d'alpinisme et d'escalade - Cordes dynamiques - Exigences de sécurité et méthodes d'essai* - Jan.2005.
- [11.3] NF S52-106 - *Pistes de ski - Fabrication des filets pour dispositif de protection* – May 2003.
- [11.4] NF EN 1891 - *Equipement de protection individuelle pour la prévention des chutes de hauteur Cordes tressées gainées à faible coefficient d'allongement* - Aug.1998.
- [11.5] DIN EN 1263 *Safety nets - Part 1 : Safety requirements, test methods* - July 2002. *Part 2: Safety requirements for the positioning limits,* Nov.2002.

[12] J.O. Hallquist, *LS-DYNA Manuals*.
- [12.1] *Keyword User's Manual, V970* – LSTC, Apr.2003.
- [12.2] *Theoretical Manual* – LSTC, May 1998.

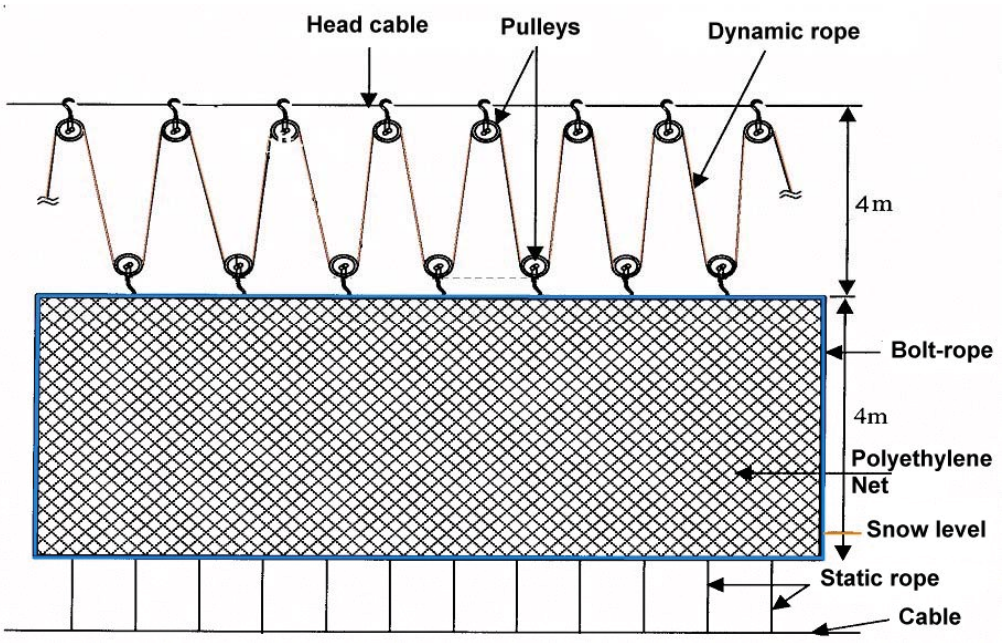


Figure 1 : General net configuration

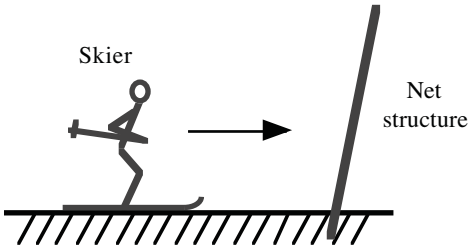


Figure 2 : Net general inclination

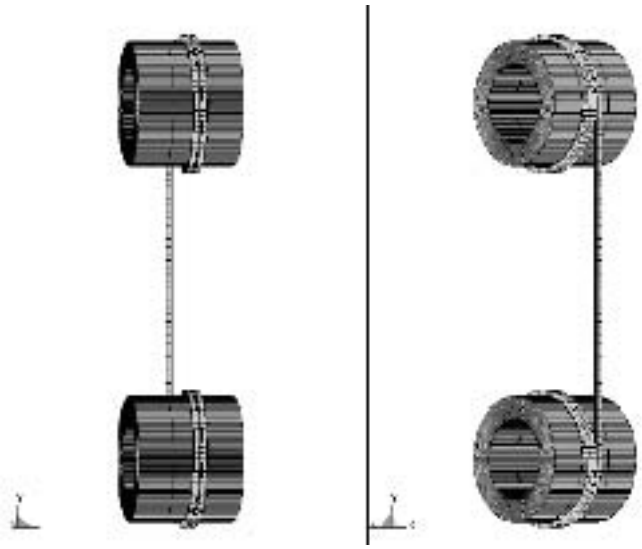

Figure 3 : Explicit model of tensile test

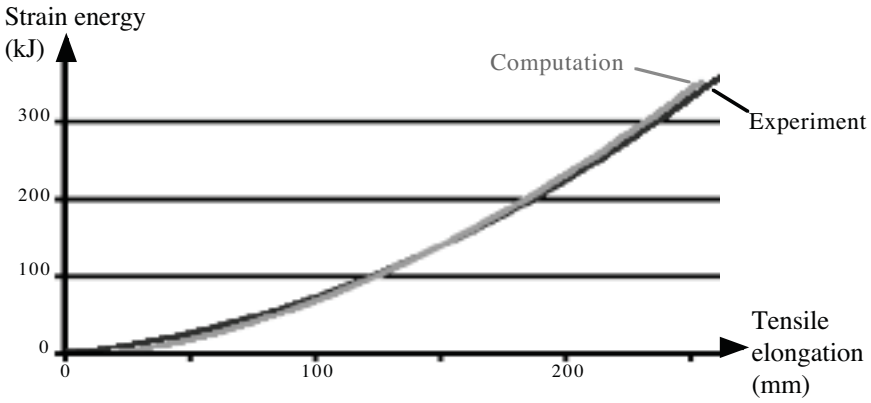


Figure 4 : Absorbed energy in 350 mm long polyethylene cord

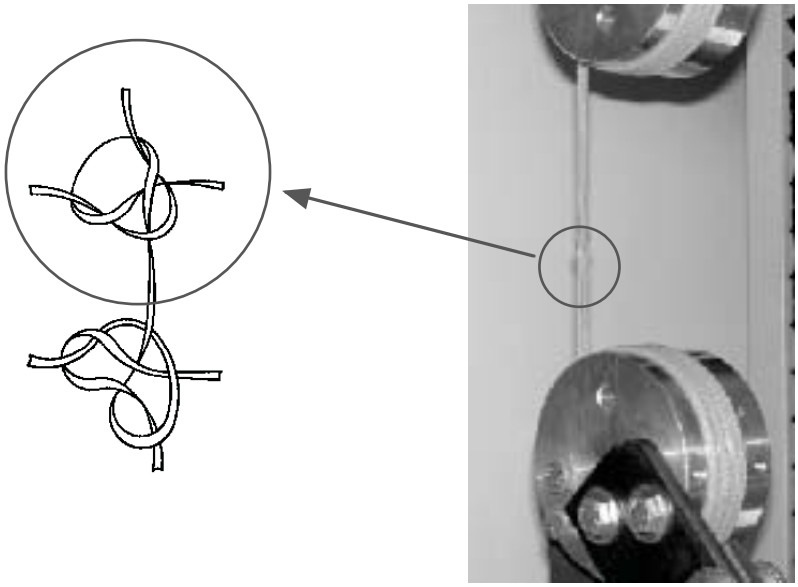

Figure 5 : Test performed on aged and knoted cord

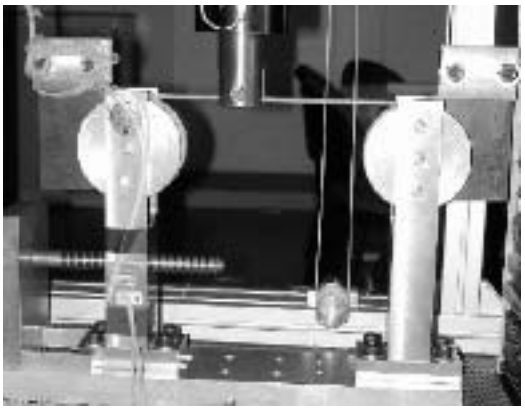

Figure 6 : Impact device for dynamical test of cords

Figure 7 : Numerical explicit model of dynamical test

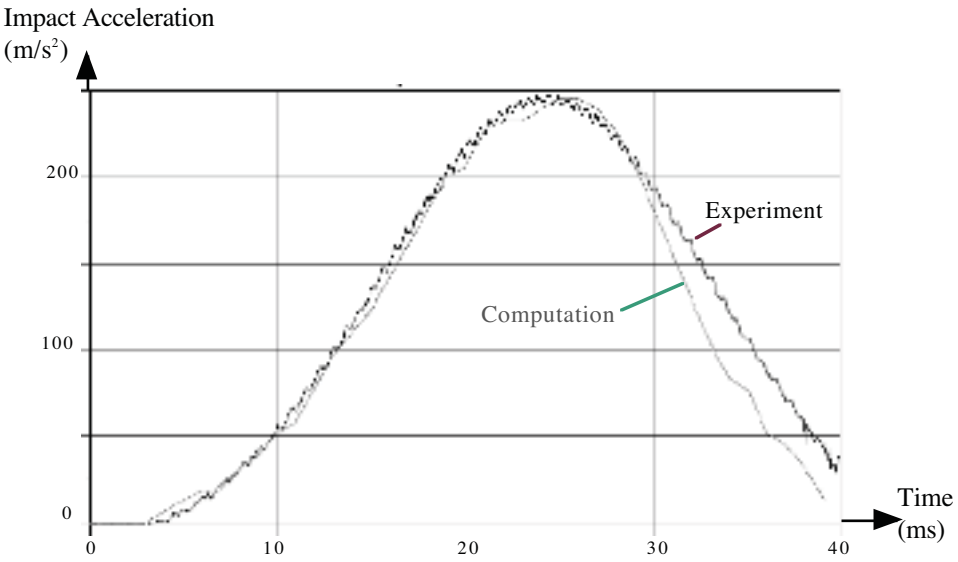


Figure 8 : Numerical explicit model of dynamical test

Figure 9 : Full-scale 3mx3m net test

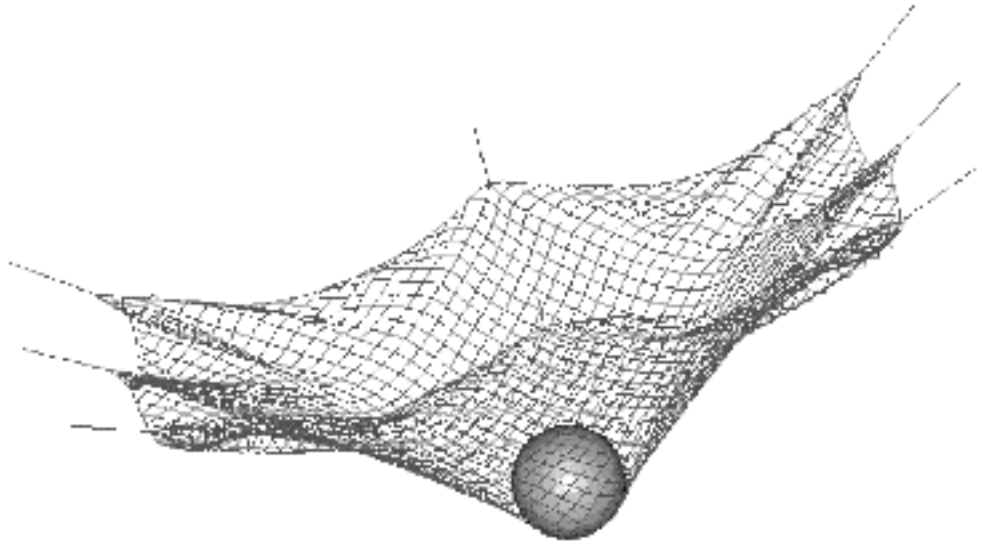

Figure 10 : Full-scale 3mx3m net model (9.5 m/s)

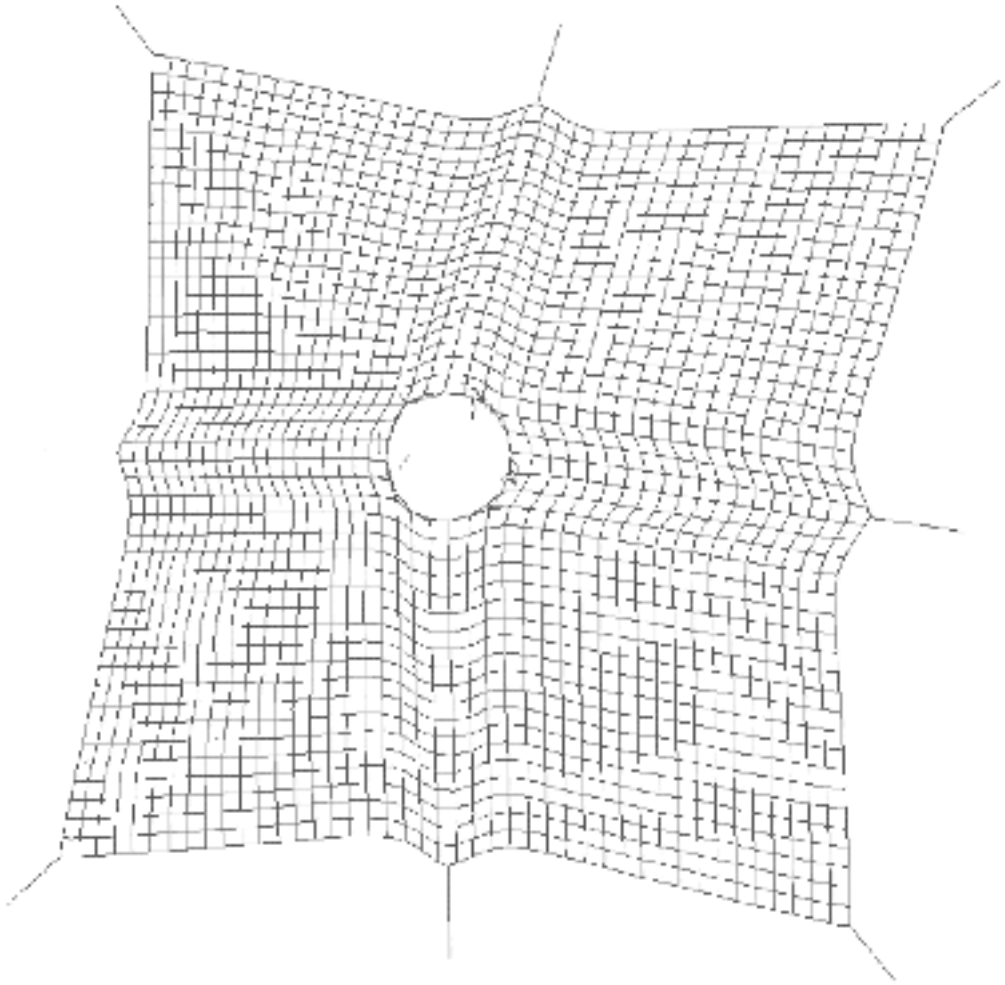

Figure 11 : Failure obtained at 9.90 m/s

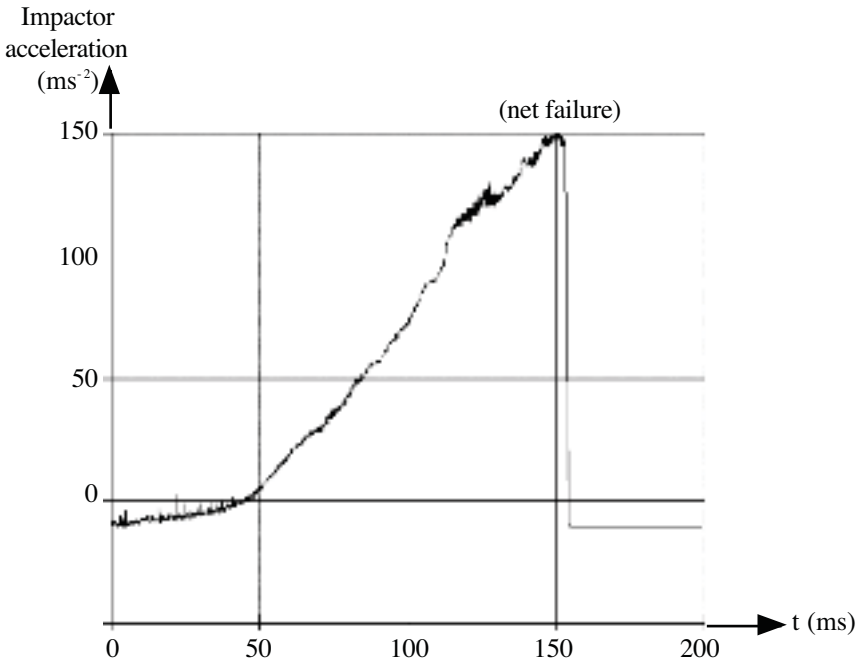


Figure 12 : Acceleration profile computed at 9.90 m/s

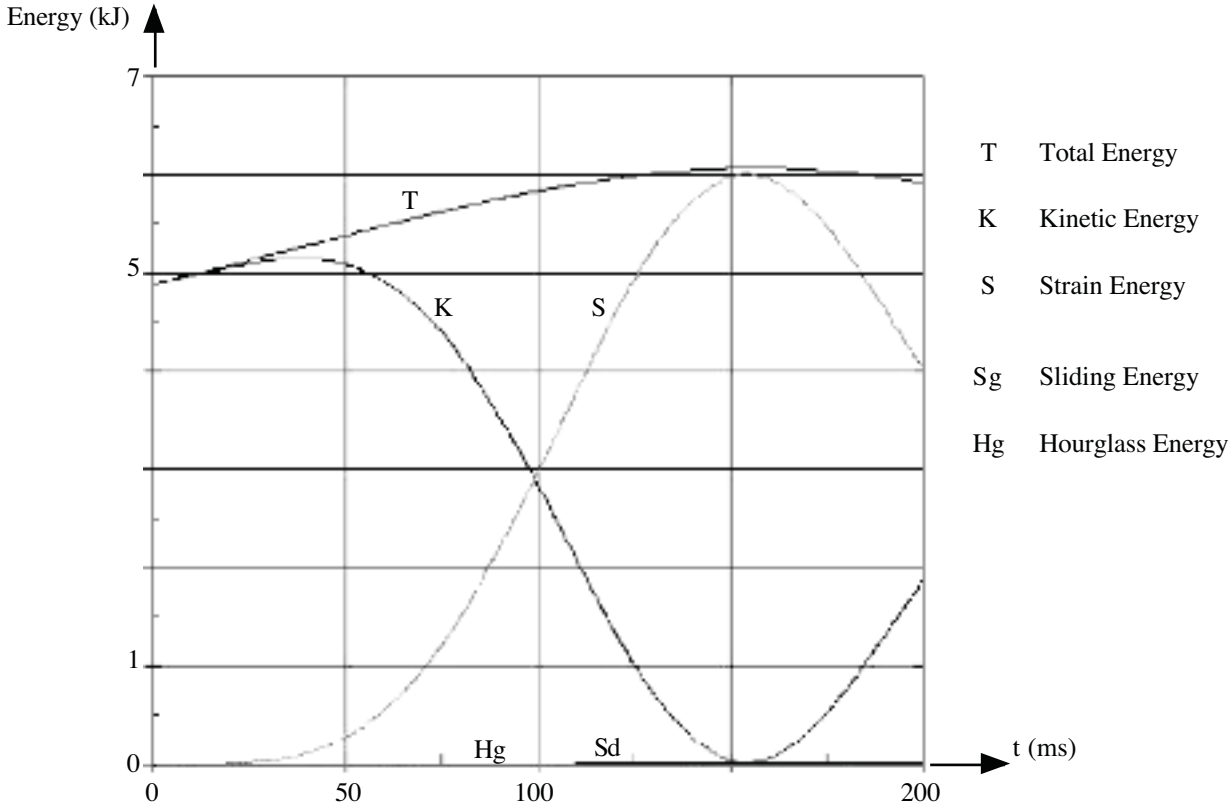


Figure 13 : Case #2S computed energies

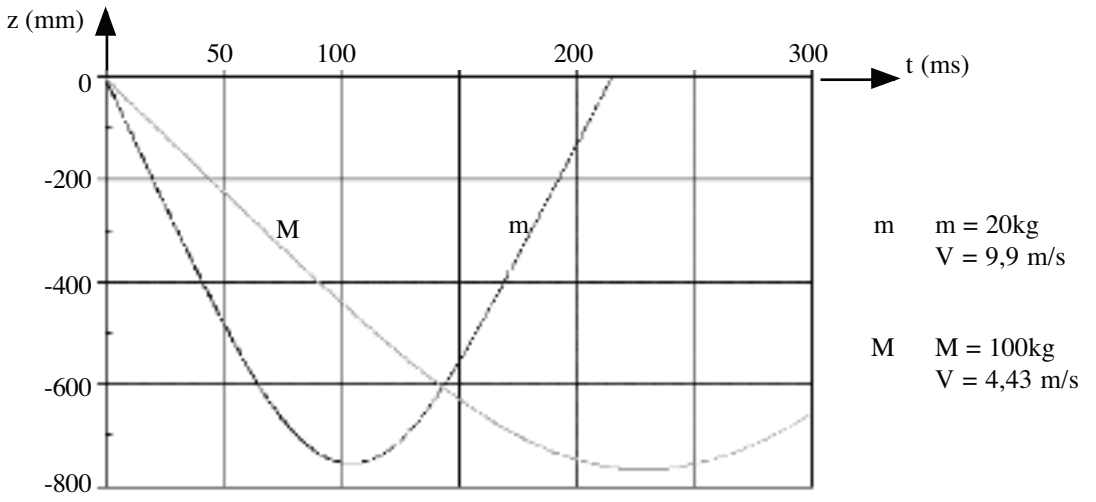


Figure 14 : Cases #3L and #3H compared deflections

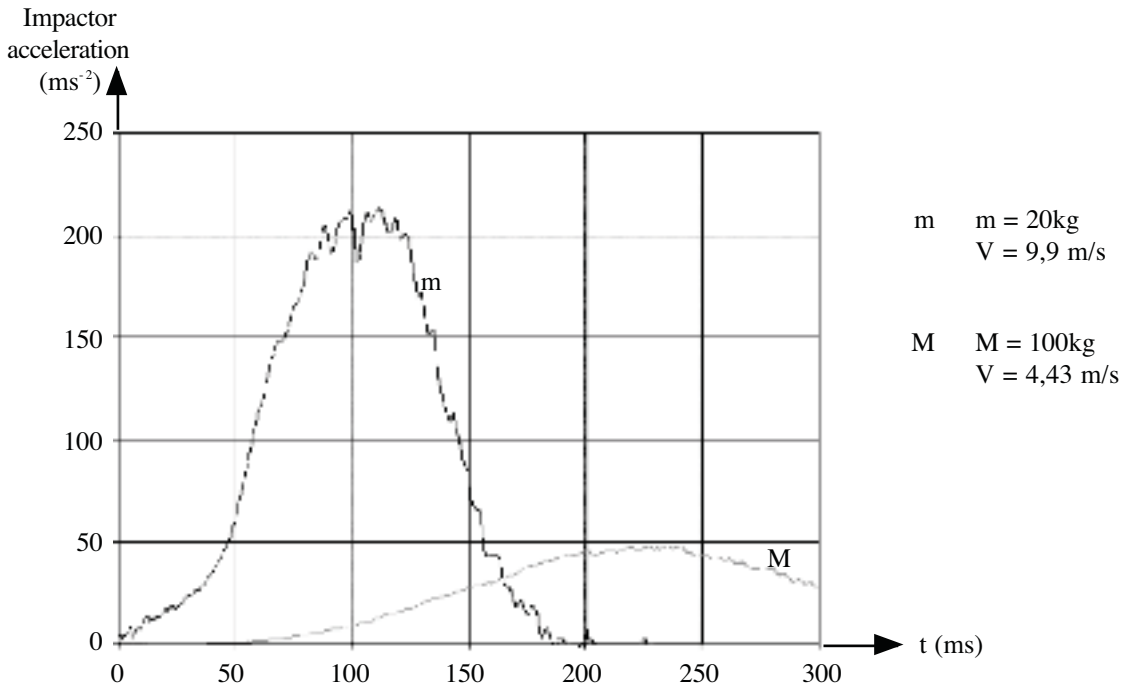


Figure 15 : Cases #3L and #3H compared accelerations

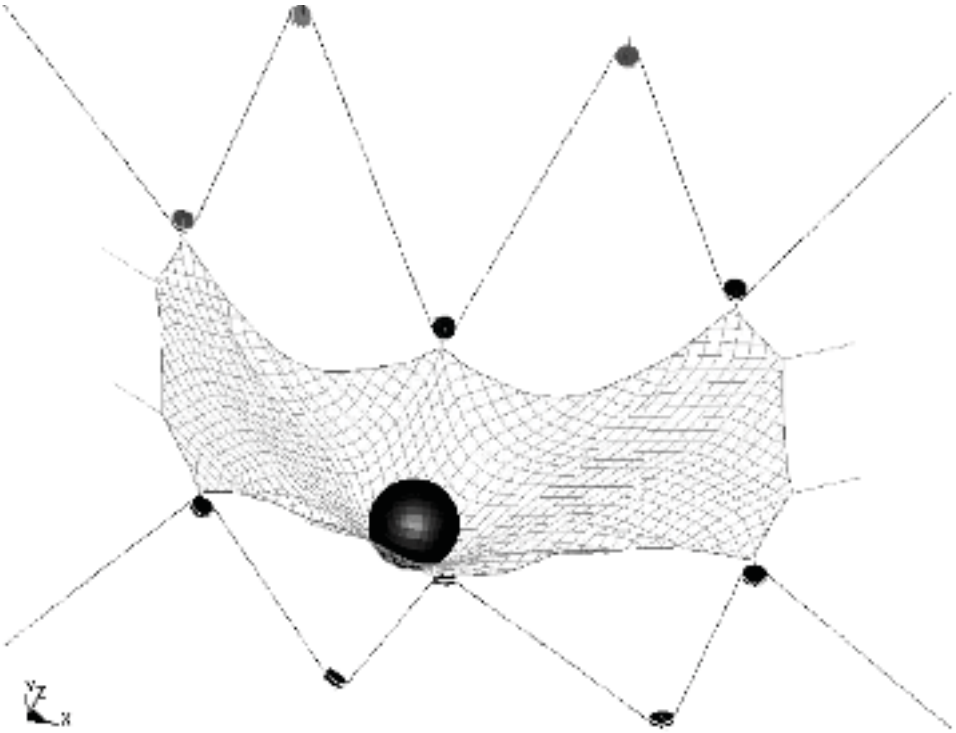

Figure 16 : Case #4R model

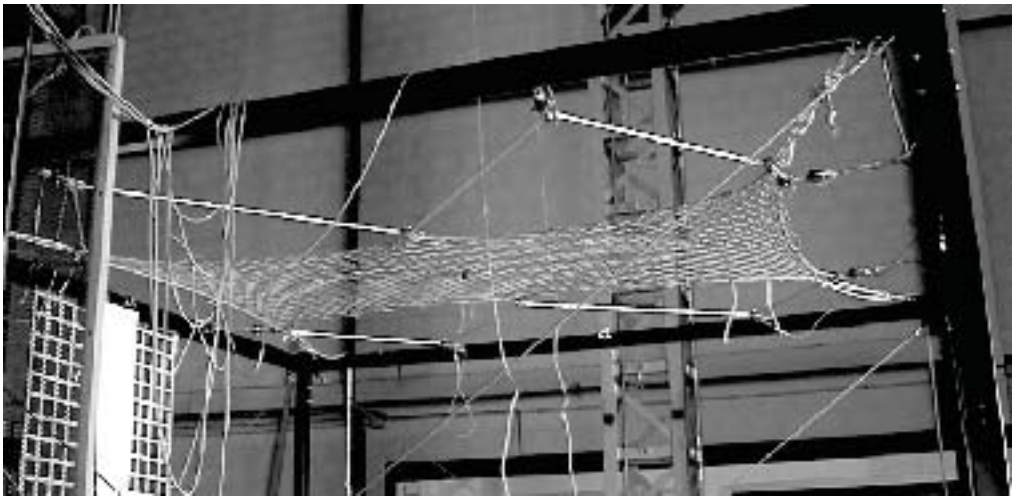

Figure 17 : Case #4R test configuration

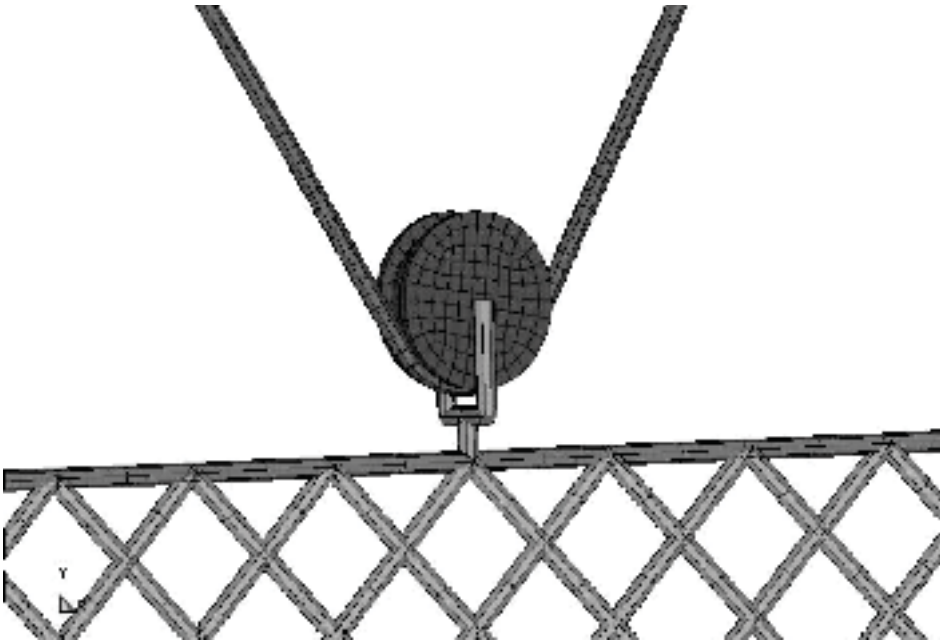

Figure 18 : Case #4R model detail (pulley and net edge)

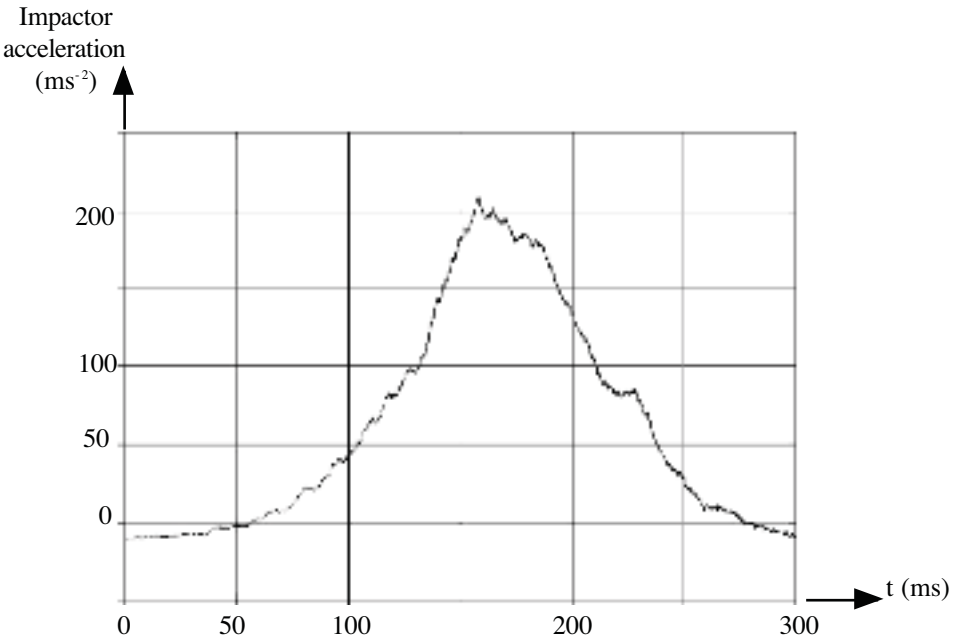


Figure 19 : Case #4R computed accelerations

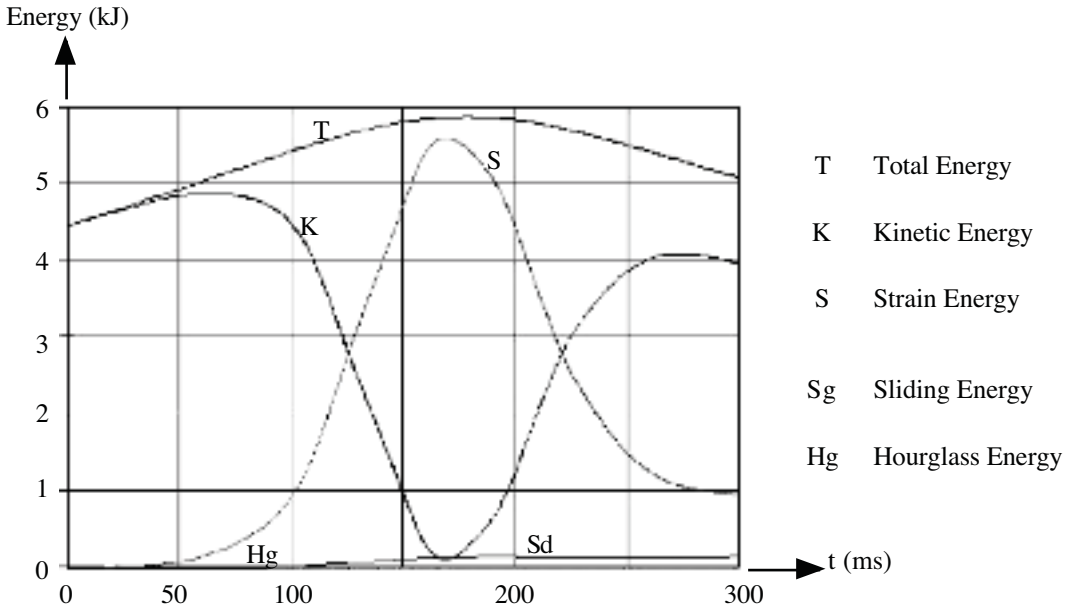


Figure 20 : Case #4R computed energies

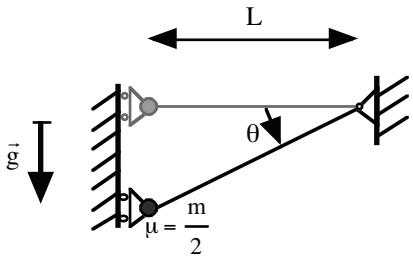


Figure 21 : Geometrical non-linearity in displacement.

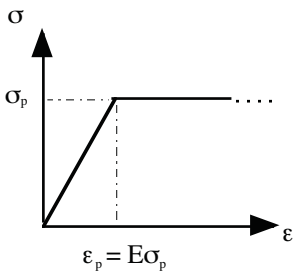


Figure 22 : Plastic curve with stress truncation.

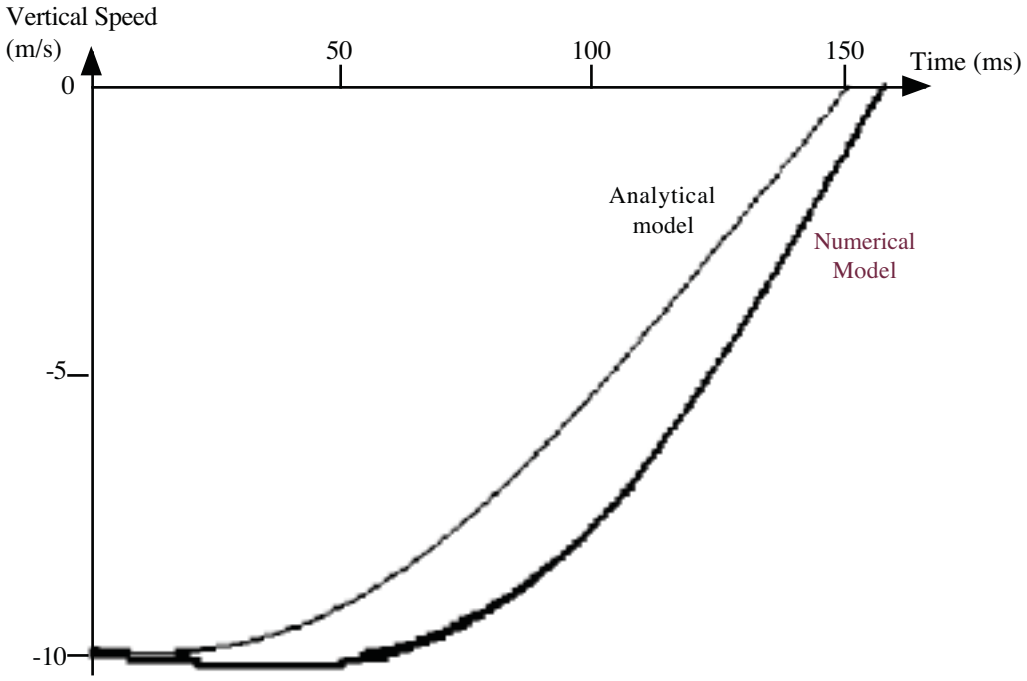


Figure 23 : Analytical and numerical speed computations